The Unified Transform: A Spectral Collocation Method for Acoustic Scattering

Lorna J. Ayton* and Matthew J Colbrook † and Athanassios S. Fokas ‡
Department of Applied Mathematics and Theoretical Physics,
University of Cambridge, CB3 0WA, UK

This paper employs the unified transform to present a boundary-based spectral collocation method suitable for solving acoustic scattering problems. The method is suitable for both interior and exterior scattering problems, and may be extended to three dimensions. A number of simple two-dimensional examples are presented to illustrate the versatility of this method, and, upon comparison with other spectral methods, or boundary-based methods the approach presented in this paper is shown to be very competitive.

I. Introduction

Acoustic scattering problems arise in a wide number of applications in the aviation industry, for example the propagation of sound along ducts, and in calculating trailing-edge noise through use of the reciprocal theorem. Often the scattered field is calculated using a boundary element method (BEM), however these are typically slow to run as they require a large number of boundary elements and thus converge only algebraically.[1] As the geometry of the scatterer becomes more complicated, computational time and storage requirements increase and new techniques are sought to reduce these costs. In the case of a periodic scatterer, recently Karimi et al[2] exploited the Toeplitz structure of the discretised system to provide a BEM which reduced computational time from $O(N^{2.66})$ to $O(N^{1.31})$. Further recent advances of BEM for acoustic scattering are discussed by Chandler-Wilde & Langdon,[4] with a particular focus toward high frequency scattering, which can often be problematic.

An alternative to a BEM is a spectral method, discussed in early work for acoustic scattering by Hwang,[3] or more generally by Trefethen,[5] which provides good accuracy for relatively few basis functions due to exponential convergence. An important first step in spectral methods is singularity removal, which is often achieved through a coordinate transformation (BEM similarly encounters problems with singularities in particular the numerical evaluation of singular integrals). For complex geometries however, it is often not possible to transform away the singularities in a traditional spectral approach and calculation of singular integrals is unavoidable.

This paper therefore presents a spectral collocation method for acoustic scattering which does not encounter problems from singularities, is suitable for high-frequency calculations, and, as it is boundary-based, is very computationally competitive. The method implements the unified transform[6] for the Helmholtz equation to derive a so-called global relation relating transforms of known and unknown boundary data in spectral space. By expanding unknown data in an appropriately chosen basis and evaluating the global relation at suitably chosen collocation points, the unknown expansion coefficients can be swiftly calculated.

The method is illustrated first for the simple problem of acoustic scattering by a finite rigid flat plate[7] , for which a fully analytic solution is known in terms of Mathieu functions.[8] Results are then given for acoustic scattering by a finite elastic plate, and quadrupole scattering by rigid plates with finite elastic extensions.

*AIAA Member, EPSRC Early Career Fellow, L.J.Ayton@damtp.cam.ac.uk
†PhD Student, St. John's College, M.Colbrook@damtp.cam.ac.uk
‡EPSRC Senior Career Fellow

II. The Unified Transform Method

A. Deriving the Global Relation

For an acoustic scattering problem, with scattered field $q(x, y)$ due to some incident field $q_{inc}(x, y)$, we must derive the global relation for the Helmholtz equation,

$$\frac{\partial^2 q}{\partial x^2} + \frac{\partial^2 q}{\partial y^2} + k_0^2 q = 0. \tag{1}$$

We suppose the domain over which the equation is to be solved, $\mathcal{D}$, is the interior of a polygon with boundary $\partial\mathcal{D}$. The domain $\mathcal{D}$ may be finite or infinite. [a]

Let v be a solution to the adjoint of the Helmholtz equation (also the Helmholtz equation). Multiplying the Helmholtz equation by v, and then subtracting the same equation with q and v interchanged yields

$$\frac{\partial}{\partial x}\left(v\frac{\partial q}{\partial x} - q\frac{\partial v}{\partial x}\right) + \frac{\partial}{\partial y}\left(v\frac{\partial q}{\partial y} - q\frac{\partial v}{\partial y}\right) = 0. \tag{2}$$

Then, Green's theorem implies

$$\int_{\partial\mathcal{D}} \left[\left(v\frac{\partial q}{\partial x} - q\frac{\partial v}{\partial x}\right)dy - \left(v\frac{\partial q}{\partial y} - q\frac{\partial v}{\partial y}\right)dx\right] = 0. \tag{3}$$

We now must include boundary conditions, therefore we parameterize $q(x, y)$ and $v(x, y)$ in terms of the arc length, s, of $\partial\mathcal{D}$. Differentiating the function $q(x(s), y(s))$ with respect to s we find

$$\frac{\partial q}{\partial x}dx + \frac{\partial q}{\partial y}dy = q_T ds, \tag{4}$$

where q_T denotes the derivative of q along the tangential direction. Thus,

$$\frac{\partial q}{\partial x}dy - \frac{\partial q}{\partial y}dx = q_n ds, \tag{5}$$

where q_n denotes the derivative of q along the outward normal to the boundary. Inserting (5) into (3) we find

$$\int_{\partial\mathcal{D}} \left(v\frac{\partial q}{\partial n} - q\frac{\partial v}{\partial n}\right)ds = 0, \tag{6}$$

where v is any solution to the (adjoint) Helmholtz equation.

In what follows, in order to further simplify the global relation, we introduce the complex variable $z = x + \mathrm{i}y$, and its conjugate $\bar{z} = x - \mathrm{i}y$. This enables us to write the Helmholtz equation in the form

$$\frac{\partial^2 q}{\partial z \partial \bar{z}} + \beta^2 q = 0, \tag{7}$$

where $\beta = k_0/2$. We choose the following particular adjoint solution,

$$v = \mathrm{e}^{-\mathrm{i}\beta(\lambda z + \frac{\bar{z}}{\lambda})}. \tag{8}$$

Then, (6) gives the global relation

$$\int_{\partial\mathcal{D}} \mathrm{e}^{-\mathrm{i}\beta(\lambda z + \frac{\bar{z}}{\lambda})}\left[q_n + \beta\left(\lambda\frac{dz}{ds} - \frac{1}{\lambda}\frac{d\bar{z}}{ds}\right)q\right]ds = 0, \qquad \lambda \in \Lambda;, \tag{9}$$

where Λ is a domain containing all λ such that the integral converges (which depends on how $\mathcal{D}$ behaves at infinity if it is unbounded, and the conditions satisfied by q at infinity).

The global relation (9) may be used directly, however to simplify it in the case of a polygonal domain where $\partial\mathcal{D}$ consists of M straight sides, we let q^j and q_n^j denote the Dirichlet and Neumann boundary values

[a] Whilst here we discuss convex polygons, for extensions to non-convex polygons one should consult Colbrook et al.[9] The unified transform can also be used for circular domains[10–12] and non-polygonal domains with general curved edges.[13]

on the j^{th} side which connects corners z_j and z_{j+1}. We then expand q^j and q_n^j in terms of a set of basis functions, $S_l(t)$:

$$q^j(t) \approx \sum_{l=0}^{N-1} a_l^j S_l(t), \qquad q_n^j(t) \approx \sum_{l=0}^{N-1} b_l^j T_l(t), \tag{10}$$

where t provides a suitable parameterisation of $\partial\mathcal{D}$, and $S_l(t)$ are a complete basis, chosen to suit the problem at hand. For example, for acoustic scattering in an unbounded domain, functions are oscillatory therefore Bessel functions of integer and half-integer order are beneficial.

Substituting the function expansions into the global relation for Helmholtz, (9), yields

$$\sum_{j=1}^{M}\sum_{l=0}^{N-1} \mathrm{e}^{-\mathrm{i}\beta(\bar{m}_j/\lambda+\lambda m_j)}\left[a_l^j\beta\left(\lambda h_j - \frac{\bar{h}_j}{\lambda}\right)\right]\hat{S}_l\left[\mathrm{i}\beta\left(\frac{\bar{h}_j}{\lambda}+\lambda h_j\right)\right]$$
$$+\sum_{j=1}^{M}\sum_{l=0}^{N-1} \mathrm{e}^{-\mathrm{i}\beta(\bar{m}_j/\lambda+\lambda m_j)} b_l^j|h_j|\hat{T}_l\left[\mathrm{i}\beta\left(\frac{\bar{h}_j}{\lambda}+\lambda h_j\right)\right] = 0,$$

for $\lambda \in \Lambda$, where $\hat{}$ is defined via

$$\hat{F}_l(\lambda) = \int_0^1 \mathrm{e}^{\mathrm{i}\lambda t} F_l(t)dt, \qquad \lambda \in \mathbb{C}, \tag{11}$$

which is consistent with previous work.[14] For any given scattering problem, some of the constants $\{a_j, b_j\}$ are known, and some unknown. By evaluating the approximate global relation at suitably chosen points collocation points we can construct sufficiently many equations to solve for the unknown constants $\{a_j, b_j\}$.

B. Problems involving multiple domains

For scattering in the interior of a convex polygon, a single global relation arises as given in the previous subsection. However for external scattering problems, multiple domains will be required. For example, scattering by a finite plate occupying $x \in [0,1]$, $y = 0$; in this case one domain is chosen as $\mathcal{D}_1 = \{y \geq 0, x \in (-\infty, \infty)\}$ and the other, $\mathcal{D}_2 = \{y \leq 0, x \in (-\infty, \infty)\}$. The boundaries, $\partial\mathcal{D}_{1,2}$, thus cover all scattering boundaries (above and below the plate).

Within each convex domain $\mathcal{D}_i$ we obtain a global relation (9) valid for $\lambda \in \Lambda_i$ (which may be different). We combine the global relations by imposing continuity of q across any shared boundaries of $\mathcal{D}_i$ which do not contain the scatterer (in the case of the finite plate, continuity across $y = 0, x < 0$ and $y = 0, x > 1$). This results in a single global relation, to which we can apply the approximations (10). This process shall be illustrated explicitly for a finite flat plate in the following section.

III. Example: finite rigid plate

Consider the scattering of an acoustic incident wave with potential

$$q_{inc} = \mathrm{e}^{\mathrm{i}k_0\cos\theta x - \mathrm{i}k_0\sin\theta y} \tag{12}$$

by a finite flat plate occupying the region $y = 0, 0 < x < 1$. The scattered potential field, q, satisfies

$$\frac{\partial^2 q}{\partial x^2} + \frac{\partial^2 q}{\partial y^2} + k_0^2 q = 0. \tag{13}$$

subject to

$$\frac{\partial q}{\partial y}(x, 0_\pm) = f(x) = \mathrm{i}k_0\sin\theta \mathrm{e}^{\mathrm{i}k_0\cos\theta x} \qquad 0 < x < 1, \tag{14}$$

and the Sommerfeld radiation condition.

We take two convex domains, $\mathcal{D}_1 = \{y \geq 0, x \in (-\infty, \infty)\}$ and $\mathcal{D}_2 = \{y \leq 0, x \in (-\infty, \infty)\}$, over which we apply the unified transform. We impose continuity across the shared boundaries;

$$\Delta q(x, 0) = 0, \qquad x < 0 \quad \text{and} \quad x > 1, \tag{15}$$

where Δq denotes the jump in q, $\Delta q(x, 0) = q(x, 0_+) - q(x, 0_-)$.

A. Global relation

Applying (9) in $\mathcal{D}_1$ we obtain

$$\begin{aligned}&\int_{-\infty}^{0} \mathrm{e}^{-\mathrm{i}\beta x(\lambda+\frac{1}{\lambda})}\left[-q_y(x,0_+)+\beta\left(\lambda-\frac{1}{\lambda}\right)q(x,0_+)\right]dx\\&+\int_{0}^{1} \mathrm{e}^{-\mathrm{i}\beta x(\lambda+\frac{1}{\lambda})}\left[-f(x)+\beta\left(\lambda-\frac{1}{\lambda}\right)q(x,0_+)\right]dx\\&+\int_{1}^{\infty} \mathrm{e}^{-\mathrm{i}\beta x(\lambda+\frac{1}{\lambda})}\left[-q_y(x,0_+)+\beta\left(\lambda-\frac{1}{\lambda}\right)q(x,0_+)\right]dx=0,\end{aligned}\tag{16}$$

where $\beta = k_0/2$. This is valid for $\lambda \in (-\infty,-1)\cup(0,1)\cup\{\mathrm{e}^{\mathrm{i}\theta}:0<\theta<\pi\}=\Lambda_1$. Similarly in $\mathcal{D}_2$ we obtain

$$\begin{aligned}&\int_{-\infty}^{0} \mathrm{e}^{-\mathrm{i}\beta x(\lambda+\frac{1}{\lambda})}\left[q_y(x,0_-)-\beta\left(\lambda-\frac{1}{\lambda}\right)q(x,0_-)\right]dx\\&+\int_{0}^{1} \mathrm{e}^{-\mathrm{i}\beta x(\lambda+\frac{1}{\lambda})}\left[f(x)-\beta\left(\lambda-\frac{1}{\lambda}\right)q(x,0_-)\right]dx\\&+\int_{1}^{\infty} \mathrm{e}^{-\mathrm{i}\beta x(\lambda+\frac{1}{\lambda})}\left[q_y(x,0_-)-\beta\left(\lambda-\frac{1}{\lambda}\right)q(x,0_-)\right]dx=0,\end{aligned}\tag{17}$$

valid for $\lambda \in (-1,0)\cup(1,\infty)\cup\{\mathrm{e}^{\mathrm{i}\theta}:\pi<\theta<2\pi\}=\Lambda_2$.

The real values allowed in $\Lambda_{1,2}$ are determined such that $\mathrm{e}^{-\mathrm{i}\beta(\lambda z+\frac{z}{\lambda})}$ converges for large $|z|$ in $\partial\mathcal{D}_{1,2}$ respectively, whilst the complex values are permitted because q satisfies the radiation condition at infinity.

We note that Λ_1 and Λ_2 are not the same, however we can apply a symmetry transform, $\lambda \to \lambda^{-1}$ which maps $\Lambda_2 \to \Lambda_1$. Under this transform (17) becomes

$$\begin{aligned}&\int_{-\infty}^{0} \mathrm{e}^{-\mathrm{i}\beta x(\lambda+\frac{1}{\lambda})}\left[q_y(x,0_-)+\beta\left(\lambda-\frac{1}{\lambda}\right)q(x,0_-)\right]dx\\&+\int_{0}^{1} \mathrm{e}^{-\mathrm{i}\beta x(\lambda+\frac{1}{\lambda})}\left[f(x)+\beta\left(\lambda-\frac{1}{\lambda}\right)q(x,0_-)\right]dx\\&+\int_{1}^{\infty} \mathrm{e}^{-\mathrm{i}\beta x(\lambda+\frac{1}{\lambda})}\left[q_y(x,0_-)+\beta\left(\lambda-\frac{1}{\lambda}\right)q(x,0_-)\right]dx=0,\end{aligned}\tag{18}$$

for $\lambda \in \Lambda_1$. We now subtract (16) from (18), and apply the continuity conditions (15) to yield our final global relation

$$\begin{aligned}&\int_{-\infty}^{0} \mathrm{e}^{-\mathrm{i}\beta x(\lambda+\frac{1}{\lambda})}q_y(x,0)dx+\int_{0}^{1} \mathrm{e}^{-\mathrm{i}\beta x(\lambda+\frac{1}{\lambda})}f(x)dx\\&+\int_{0}^{1} \mathrm{e}^{-\mathrm{i}\beta x(\lambda+\frac{1}{\lambda})}\frac{\beta}{2}\left(\lambda-\frac{1}{\lambda}\right)\Delta q(x,0)dx+\int_{1}^{\infty} \mathrm{e}^{-\mathrm{i}\beta x(\lambda+\frac{1}{\lambda})}q_y(x,0)dx=0,\end{aligned}\tag{19}$$

where we also use $q_y(x,0_+)=q_y(x,0_-)$ for $x<0$ and $x>1$.

We now set

$$q_y(-t,0)=\sum_{l=0}^{N-1} a_l S_l^1(t) \qquad t\in[0,\infty)\tag{20}$$

$$\Delta q(t,0)=\sum_{l=0}^{N-1} b_l S_l^2(t) \qquad t\in[0,1]\tag{21}$$

$$q_y(t+1,0)=\sum_{l=0}^{N-1} c_l S_l^3(t) \qquad t\in[0,\infty)\tag{22}$$

as a basis expansion of our unknown boundary data. Upon substitution into (19) we obtain

$$\sum_{l=0}^{N-1}\left\{a_l\tilde{S}_l^1\left[\beta(\lambda+\frac{1}{\lambda})\right]+\frac{\beta}{2}b_l\left(\lambda-\frac{1}{\lambda}\right)\hat{S}_l^2\left[-\beta(\lambda+\frac{1}{\lambda})\right]+\mathrm{e}^{-\mathrm{i}\beta(\lambda+\frac{1}{\lambda})}c_l\tilde{S}_l^3\left[-\beta(\lambda+\frac{1}{\lambda})\right]\right\}$$
$$=-\int_0^1\mathrm{e}^{-\mathrm{i}\beta x(\lambda+\frac{1}{\lambda})}f(x)dx,\qquad\lambda\in\Lambda_1,\tag{23}$$

where the right hand side is known (and in this case can be evaluated explicitly), and

$$\tilde{S}_l(\lambda)=\int_0^\infty\mathrm{e}^{\mathrm{i}\lambda t}S_l(t)dt.\tag{24}$$

B. Collocation points and basis choice

We first must consider what behaviour can be expected for the unknown functions involved in (23). Over the finite plate, we expect square root type behaviour of Δq close to the edges, $x=0,1$. To capture this, we use a weighted Chebyshev basis [b]

$$C_m(t)=\begin{cases}\cos(m\chi(t)), & m\text{ odd}\\ \mathrm{i}\sin(m\chi(t)), & m\text{ even}\end{cases},\tag{25}$$

where $\chi(t)=\arcsin(t)\in[0,\pi/2]$. For the semi-infinite intervals we used the Bessel functions $\{J_{\frac{n+1}{2}}(k_0x)/x\}_{n=0}^{\hat{N}-1}$ to capture the oscillatory behaviour. These also have the advantage of capturing the correct singular behaviour near the plate edges when n is even, and they decay with the correct algebraic rate at infinity.

For collocation points $\lambda\in\Lambda_1$, we chose M_1 Halton nodes in the interval (0,1), minus their reciprocal values in $(-\infty,-1)$, and M_2 points in $\{\mathrm{e}^{\mathrm{i}\theta}:0<\theta<\pi\}$ with θ corresponding to Halton nodes in $(0,\pi)$. With the change of variables $\omega=\beta(\lambda+\lambda^{-1})$, this corresponds to sampling frequencies along the entire real line of the Fourier transforms of the relevant functions.

Recall, the complex collocation points along the unit circle are allowed precisely because the solution satisfies the Sommerfeld radiation condition so that the contribution of Green's identity along the relevant semi-circular arc vanishes in the infinite radius limit[15] . To obtain accurate numerical solutions we must sample these points as this corresponds to implementing the boundary conditions that make the problem well posed.

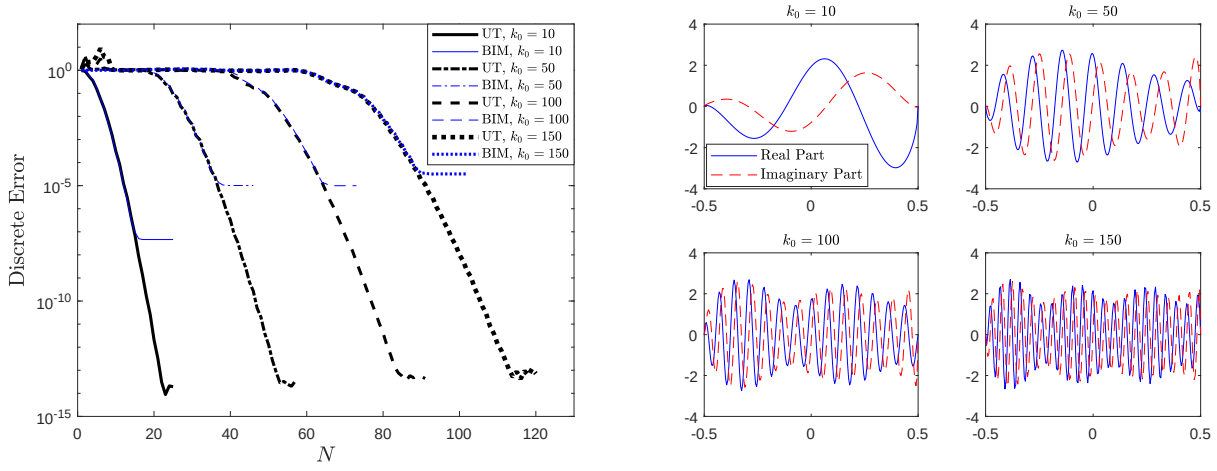

Figure 1: Left: Errors for the single plate problem. UT denotes the unified transform whereas BIM denotes the boundary integral method. Right: The analytic solutions $\Delta q(x,0)$ for different k_0.

[b] More precisely, Chebyshev polynomials of the second kind multiplied by $\sqrt{1-t^2}$.

C. Numerical results

We compare the solution for $\Delta q(x,0)$ against the known analytical solution which can be obtained in terms of Mathieu functions[16,17] to obtain a discrete error. We also compare against a classic boundary integral method.[18] Figure 1 shows the error results for the unified transform and the boundary integral method for $\theta = \pi/6$. The unified transform is able to obtain near machine precision for a wide range of wavenumbers k_0 (the required number N to gain a specified number of digits also appears to grow linearly with ${k_0}^7$), whereas the boundary integral method struggles, especially for higher frequencies. This is due to the difficulty in computing singular integrals, a difficulty which is entirely avoided when using the unified transform. The unified transform is very fast, taking a couple of seconds for $N = 120$ (corresponding to 600 basis functions).

We can, as is standard for BEMs, obtain the full scattered field by using a Green's function integral representation. We illustrate some scattered fields in Figure 2 for an incident plane wave.

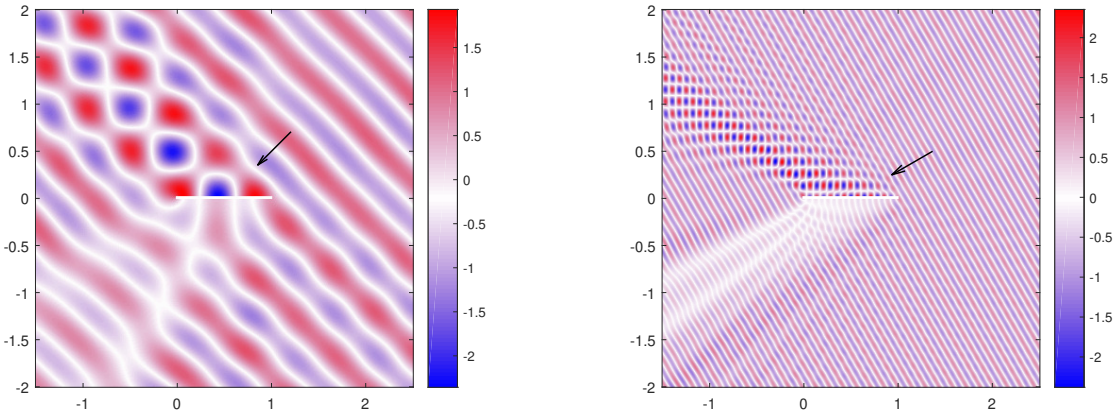

Figure 2: Real part of the total field (incident plus scattered) due to plane wave scattering off a rigid plate. Arrow denotes the direction of propagation of the incident wave. Left: $k_0 = 10$. Right: $k_0 = 50$.

IV. Example: acoustic scattering by an elastic plate

We now consider the scattering of an incident pressure field by a finite elastic plate with end points $x = 0, 1$ executing small deformations from $y = 0$. The deformation of the plate is $\eta(x)e^{-\mathrm{i}\omega t}$ (where as before, time factors will be removed throughout). The scattered field, $q(x,y)$, thus satisfies the Helmholtz equation as before, but now we require a dynamic condition in the plate;

$$\left(\frac{\partial^4}{\partial x^4} - \frac{k_0^4}{\Omega^4}\right)\eta = -\frac{\epsilon}{\Omega^6}k_0^3\Delta q \quad \text{on} \quad y = 0, \tag{26}$$

where ϵ is the fluid loading parameter, and Ω the vacuum bending wave Mach number for the plate.[19] We also require a kinematic condition;

$$k_0^2\eta = \frac{\partial q_{inc}}{\partial y} + \frac{\partial q}{\partial y} \quad \text{on} \quad y = 0. \tag{27}$$

Finally, as before, we demand continuity of q upstream and downstream of the plate along $y = 0$.

The ends of each plate will be specified as either clamped or free. Supposing the end of an elastic plate is at $x = x_0$, it is clamped if

$$\eta(x_0) = \eta'(x_0) = 0, \tag{28}$$

or it is free if

$$\eta''(x_0) = \eta'''(x_0) = 0. \tag{29}$$

In this example we shall consider the leading edge, $x = 0$, to be clamped, and the trailing edge, $x = 1$, to be free.

Since the setup of the problem in this example satisfies the same governing equation (Helmholtz), we can follow the same procedure as outlined in the previous section. As such the equivalent approximate global relation to (23) is

$$\sum_{j=1}^{N} a_j \int_{-1}^{1} \mathrm{e}^{-\mathrm{i}\beta x(\lambda+\frac{1}{\lambda})} \left[k_0^2 - \frac{\beta\Omega^6}{2k_0^3\epsilon_1}\left(d_j^4 - \frac{k_0^4}{\Omega^4}\right)\left(\lambda - \frac{1}{\lambda}\right)\right] f_j(x)dx$$
$$+ \sum_{n=1}^{2}\sum_{j=1}^{N} \hat{L}_{j,n}(\lambda)\, b_{j,n} = \int_0^1 \mathrm{e}^{-\mathrm{i}\beta x(\lambda+\frac{1}{\lambda})} \frac{\partial q_I}{\partial y}(x,0)dx,$$

where f_j and d_j are eigenfunctions and eigenvalues respectively for the ∇^4 operator (which can be calculated via standard spectral methods). Thus this expansion is equivalent to expanding the plate deformation, η, in its modal basis. The basis functions $L_{j,n}$ are, as for the rigid case, transforms of Bessel functions such that

$$\frac{\partial q}{\partial y}(-t,0) = \sum_{j=1}^{N} b_{j,1} \frac{J_{j/2}(k_0 t)}{t}, \tag{30}$$

$$\frac{\partial q}{\partial y}(t+1,0) = \sum_{j=1}^{N} b_{j,2} \frac{J_{j/2}(k_0 t)}{t}. \tag{31}$$

We illustrate some sample scattered acoustic fields in Figure 3 for various elastic plates

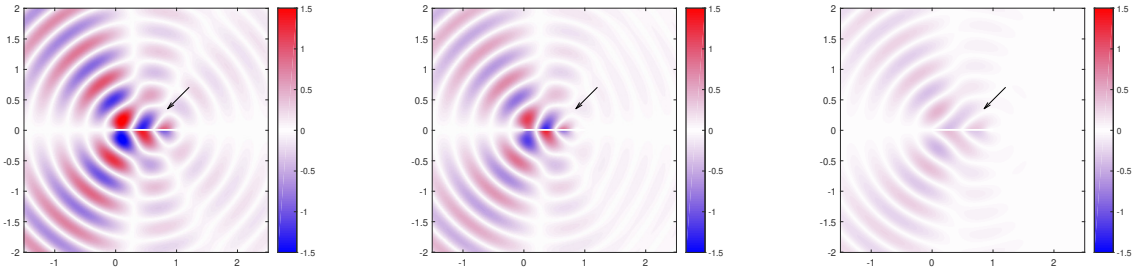

Figure 3: Real part of the scattered field due to plane wave scattering off an elastic plate with $\epsilon = 0.135$. Arrow denotes the direction of propagation of the incident wave with $k_0 = 10$. Left: rigid. Centre: $\Omega = 0.8$. Right: $\Omega = 0.4$.

V. Example: aerodynamic noise generated by a partially elastic plate

Elastic plates are known to reduce aerodynamically generated noise[19] versus rigid plates. However, practically a fully elastic plate is undesirable, thus we wish to consider the acoustic benefits of partially elastic plates.[20] In this section we thus suppose a rigid plate lies in the region $x \in [0, 1-l]$, and an elastic plate is clamped to it along $x \in [1-l, 1]$, for $l < 1$. The incident field is taken as a lateral quadrupole located close to the trailing edge.

Figure 4 illustrates the relative far-field sound power, defined as the sound power for the partially elastic plate divided by the sound power for an equivalent rigid plate, for varying l and elasticity parameter, Ω. We see clearly plates with elastic sections are beneficial in reducing noise, however resonances of the plate can lead to noise increases and are affected by the total length and flexibility of the plate, as expected. Overall this figure indicates for highly flexible plates (small Ω), a 25% elastic extent may provide significant noise reduction, more so even than plates with greater elastic extents. It could therefore be of future interest to use this method to determine an optimal aeroacoustic and aerodynamic balance for partially elastic plates.

VI. Conclusions

This paper has presented a boundary-based spectral collocation method suited to acoustic scattering problems which can significantly out perform boundary element and boundary integral methods, and due

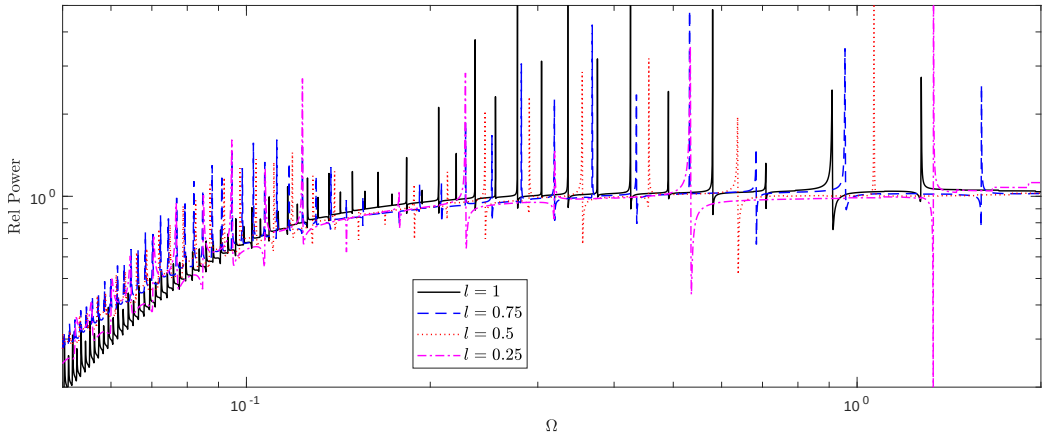

Figure 4: Relative sound power due to a lateral quadrupole scattering at the trailing edge of a partially elastic plate, for $k_0 = 10$, $\epsilon = 0.0021$.

to the approach not requiring the evaluation of singular integrals, it is competitive against other spectral methods, particularly in complex geometry domains. The method has been validated by considering the problem of an acoustic wave scattering by a finite rigid flat plate, and illustrated for the cases including plate elasticity.

Whilst formulated for polygonal domains in this paper, this method extends to more arbitrary geometries,[13] including multiple disjoint scatterers with a range of physical boundary conditions. It may also be extended to three-dimensions by allowing for two complex parameters, λ and μ during the selection of an arbitrary solution v. This however leads to much more complicated symmetry transforms and basis selection, thus work is ongoing.

Acknowledgments

This work was supported by EPSRC Early-Career Fellowship EP/P015980/1 (L.J.A.), EPSRC grant EP/L016516/1 (M.J.C), and by EPSRC Senior Fellowship EP/RG8/609 (A.S.F.).

References

[1]Unger, G. 2009 Analysis of boundary element methods for Laplacian eigenvalue problems, *Verlag der Techn. Univ. Graz*

[2]Karimi, M., Croaker, P., and Kessissoglou, N. 2016 Boundary element solution for periodic acoustic problems, *J. Sound. Vib.* **360**, 129–139.

[3]Hwang, W.S. 1997 Boundary spectral method for acoustic scattering and radiation problems, *J. Acoust. Soc. Am.* **102**, 96–101.

[4]Chandler-Wilde, S.N. and Langdon, S. 2015 Acoustic scattering : high frequency boundary element methods and unified transform methods *Unified transform for boundary value problems: applications and advances. SIAM*, 181–226.

[5]Trefethen, L.N. 2000 Spectral methods in MATLAB, *Siam*

[6]Fokas, A.S. 2008 A unified approach to boundary value problems *SIAM*

[7]Colbrook, M. J., Ayton, L. J. and Fokas, A. S. 2019 The unified transform for mixed boundary condition problems in unbounded domains *P. Roy. Soc. A* **475**, 20180605.

[8]McLachlan, N.W. 1964 Theory and application of Mathieu functions, Dover Publications

[9]Colbrook, M.J., Flyer, N. and Fornberg, B. 2018 On the Fokas method for the solution of elliptic problems in both convex and non-convex polygonal domains *J. Comput. Phys.* **374**, 996–1016

[10]Crowdy, D. 2015 Fourier–Mellin transforms for circular domains *Comput. Meth. Funct. Th.* **15**, 655–687

[11]Crowdy, D. 2015 A transform method for Laplace's equation in multiply connected circular domains, *IMA J. Appl. Math.* **80** 1902–1931

[12]Luca, E. and Crowdy, D. 2018 A transform method for the biharmonic equation in multiply connected circular domains *IMA J. Appl. Math.* hxy030

[13]Colbrook, M.J. Extending the Fokas method: Curvilinear Polygons and Variable Coefficient PDEs, (submitted)

[14]Hashemzadeh, P., Fokas, A.S. and Smitheman, S.A. 2015 A numerical technique for linear elliptic partial differential equations in polygonal domains *Proc. R. Soc. A* **471** 20140747

[15]Spence, E.A. 2011 Boundary value problems for linear elliptic PDEs PhD thesis, University of Cambridge

[16]Kisil, A. and Ayton, L.J. 2018 Aerodynamic noise generated by finite porous extensions to rigid trailing edges *J. Fluid. Mech.* **836**, 117–144

[17]Nigro, D. 2017 Prediction of broadband aero and hydrodynamic noise: derivation of analytical models for low frequency PhD thesis, University of Manchester

[18]Achenbach, J.D. and Li, Z.L. 1986 Reflection and transmission of scalar waves by a periodic array of screens *Wave motion* **8**, 225–234

[19]Cavalieri, A. V. G. Wolf, W. R. & Jaworski, J. W. 2016 Numerical solution of acoustic scattering by finite perforated elastic plates. *P. Roy. Soc. A* **427**, 20150767.

[20]Ayton, L. J. 2016 Acoustic scattering by a finite rigid plate with a poroelastic extension *Journal of Fluid Mechanics* **791**, 414 – 438.